

CERN LIBRARIES, GENEVA



SCAN-9902085

E15-98-284

R.Wolski¹, A.S.Fomichev, A.M.Rodin, S.I.Sidorchuk,
S.V.Stepantsov, G.M.Ter-Akopian, M.L.Chelnokov,
V.A.Gorshkov, A.Yu.Lavrentev, V.I.Zagrebaev,
Yu.Ts.Oganessian, P.Roussel-Chomaz², W.Mittig², I.David³

STUDY OF $1n$ AND $2n$ TRANSFER REACTIONS
IN ${}^6\text{He} + p$ SYSTEM AT 25 MeV/n ENERGY
OF ${}^6\text{He}$ BEAM

¹On leave from the Institute of Nuclear Physics, Cracow, Poland

²GANIL BP5027, Caen, France

³Institute of Atomic Physics, P.O.B. MG6 Bucharest, Romania

1. Introduction

${}^6\text{He}$ is the lightest nucleus having the two-neutron halo [1]. Experimental studies of its structure are of special interest since the three-body model [2] predicts specific configurations of valence neutrons in respect to the ${}^4\text{He}$ core in this nucleus. The properties of ${}^6\text{He}$ have been investigated by the measurements of total reaction cross-section, alpha particle and neutrons momentum distributions observed in fragmentation reactions [1], the study of ground state β decay [3] and neutron decay of excited states in a kinematically complete experiment [4].

Transfer reactions are known as a good tool to extract spectroscopic parameters of simple nuclear configurations. It seems to be natural to extend that approach for the case of exotic halo nuclei. For obvious reasons, data on transfer reactions with radioactive beams are scarce. The quality of presently available radioactive beams does not match the usual requirements for measuring of angular distributions for transfer processes. Recently we observed the 2-n transfer reaction in backward angle elastic scattering in the ${}^6\text{He} + {}^4\text{He}$ system [5]. The large spectroscopic factor for the $\alpha + 2n$ configuration has been obtained confirming the expectation of the three-body model [2]. Analogously, the high degree of d- α clustering has been experimentally established for ${}^6\text{Li}$ nucleus. According to the shell model calculations both ${}^6\text{He}$ and ${}^6\text{Li}$ nuclei are characterized with large spectroscopic amplitudes for $\alpha + 2n$ and $\alpha + d$ as well as t+t and ${}^3\text{He} + t$ configurations respectively, see for example Ref. [6]. Several experimental data, e.g. elastic scattering at backward angles in the ${}^6\text{Li} + {}^3\text{He}$ system, (see, for instance, [7]), transfer reaction in ${}^6\text{Li} + p$ [8] and ${}^6\text{Li} + n$ [9] systems, do endorse the significance of the three nucleon clusters in ${}^6\text{Li}$ nucleus. The similar picture could be expected for ${}^6\text{He}$ nucleus.

We have performed the measurements of angular distributions for the transfer reaction and the elastic channels for the ${}^6\text{He} + p$ system using inverse kinematics with a ${}^6\text{He}$ radioactive beam. This is the rarely investigated case of the transfer process with halo and non-halo nuclei being involved. Having in mind the corresponding data for the ${}^6\text{Li} + p$ system one could compare the influence of the structural parameters of these two nuclei on the processes studied. The angular distributions of the elastic scattering and of 1n and 2n transfer reactions were obtained by coincidence measurement of kinetic energy of both reaction partners.

2. Experiment

The secondary beam of ${}^6\text{He}$ nuclei was produced by the bombardment of a thick (350 mg/cm²) beryllium target with a 43 MeV/n ${}^{13}\text{C}$ primary beam. The ${}^6\text{He}$ ions were separated from the primary beam particles and main part of other reaction products using doubly achromatic separator – ACCULINNA described elsewhere [10]. A wedge-shape Al plate was used in the intermediate focal plane of ACCULINNA. Eventually, the secondary ${}^6\text{He}$ beam of 150 MeV energy and 5% energy resolution (FMHW) was collimated to the diameter of ~8mm by Al diaphragms limiting the beam spot on a target. The average beam intensity amounted up to 1×10^5 of ${}^6\text{He}$ particles per second. The main parasite components of the beam were ${}^8\text{Li}$ ions ~20% and tritons ~50%. The composition of the beam and its intensity were monitored by the system of two plastic scintillators, a thin one (150 μm) placed between the diaphragms and another thick plastic placed downstream against the beam, see Fig. 1. A 400 μm CH₂ foil was used as the hydrogen target.

Reaction products of interest were detected by a system of two $\Delta E \times \Delta E \times E$ telescopes mounted on two movable arms in the horizontal plane. Each telescope consisted of two silicon strip detectors (area – 60 \times 60 mm², thickness – 400 μm , 29 identical 2 mm strips in each detector) and a 20mm thick CsJ(Tl) crystal of 65 \times 65mm² in area. The strip detectors provided both X and Y position and ΔE signals, and the thick detector supplied E signals. Both halves of each strip detector, e.g. 14 (15) strips were connected through resistors and operated in the charge division mode. This way, the volume of electronics was greatly reduced without loss in the position resolution. However the procedure generated a weak position amplitude dependence of the ΔE signal. To remedy this effect

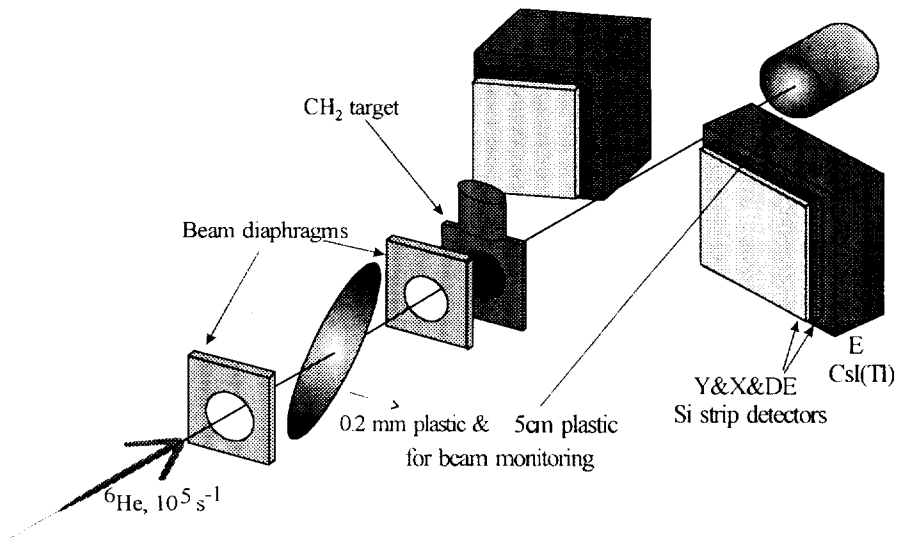


Fig. 1 Beam diaphragms, CH₂ target and detector array

a careful off line calibration of the strip detectors was carried out using an alpha particle source, and the appropriate corrections were derived. The telescopes were also calibrated on line by detection of low intensity beams of protons, deuterons, tritons, α particles and ${}^6\text{He}$ ions at several projectile energies. The beams were provided by ACCULINNA. The overall energy resolution of the telescopes was estimated to be $\sim 2\%$.

In order to subtend large solid angles the telescopes were installed in the distances of 10.5 cm and 12.5 cm from the target. This compact geometry and the high radiation level in the experimental area caused a large background, mainly of non-target origin. The background made impossible the observation of inclusive spectra of reaction products. The coincident events corresponding to the three reaction exit channels: ${}^6\text{He} + p$, ${}^5\text{He} + d$, and $\alpha + t$ were collected under condition that one telescope being a master opened the time gate (5 μs) of the data acquisition system. The second telescope was a slave. Due to the fact, that all excited states of the nuclei in question are particle unstable the identification of both participants for each binary reaction allowed determining uniquely the reaction channel. The only exception is the ${}^5\text{He} + d$ reaction where a small yield of the $\alpha + d + n$ exit channel was expected to contribute in that part of the deuteron coincidence spectrum, which corresponds to the $p_{3/2}$ ground state of ${}^5\text{He}$.

The data were collected in two runs, in which different angular ranges of the telescopes were set:

- 1) Symmetrical intended mainly for the $\alpha + t$ exit channel. The centers of the telescopes were placed at laboratory angles of 22° (slave) and 23° (master).

2) Asymmetrical dedicated to the measurement of elastic scattering angular distribution. Angle setting (laboratory system): 19° (slave) and 51° (master).

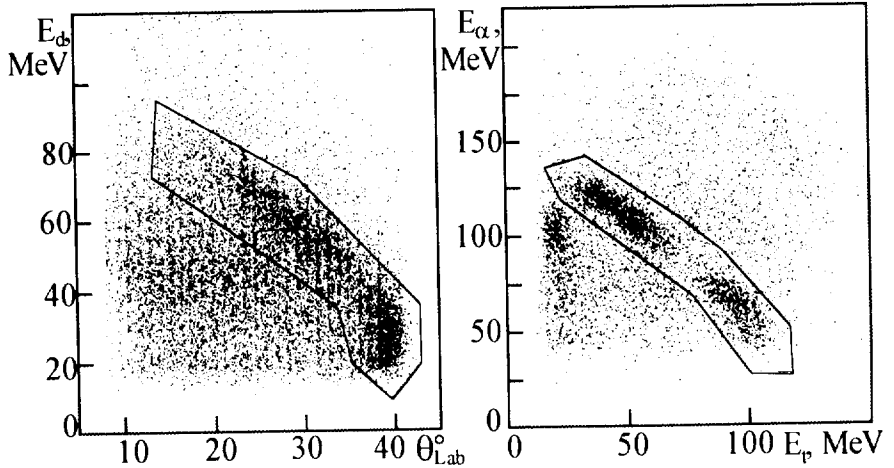


Fig. 2. Two dimension spectra: a) deuteron energy versus deuteron LAB angle for the ${}^5\text{He} + d$ exit channel, b) α particle energy versus triton energy for $\alpha + t$ exit channel. Contour lines indicate the loci for these reaction channels in the plots.

Fig. 2a shows two-dimension spectrum of deuterons obtained in one telescope in coincidence with α particles detected in the second one. Fig. 2b shows the energy correlation between alpha particles detected in one telescope versus the energy of tritons observed in the second one. In each case the kinematical loci are clearly visible. The locus of the correlated proton - ${}^6\text{He}$ events (not shown here) is even more prominent.

Angular distributions for $p({}^6\text{He}, {}^6\text{He})p$ and $p({}^6\text{He}, \alpha)t$ reactions were extracted from the spectra of the type shown in Fig. 2b. Taking into account the poor angular resolution caused by the large beam spot on the target the values of CM scattering angle were derived by the energy balance of both reaction partners. The angular distribution for the $p({}^6\text{He}, {}^5\text{He})d$ reaction was created on a basis of the energy-angle bins dissection of the spectrum seen in Fig. 2a. The method of extracting the angular distributions implies that the angular resolution is not higher than the spacing of angular distributions points, which show the angular distribution patterns, i.e. 5° in CM in most cases.

The differential cross-sections extracted for the tree channels were corrected by means of efficiency functions. The Monte Carlo simulations of experimental conditions were performed to evaluate the efficiency factor for all angular bins of the studied reaction channels. The simulations took into account the telescope solid angles limitations, beam energy spread, the finite size of the beam spot on the target and detector energy thresholds. In the special case of the ground state ${}^5\text{He}$ decay the sharp level energy and isotropic decay were assumed

For the elastic and $1n$ transfer reaction channels the presently attained angular distribution data were supplemented by experimental points obtained in a preliminary experiment, which we carried out earlier. In this experiment, we applied two Si-detector telescopes. The experimental equipment and ${}^6\text{He}$ -beam quality are described in details in ref. [5]. The same CH_2 target was used and the angular setting of the telescopes was in lab. system. 12° (master) and 32° (slave). We

extracted from this early experiment elastic scattering data for a CM angular range extending from 95° to 135° . These data were obtained from the single ${}^6\text{He}$ -energy spectrum. In the same run the angular distribution of $p({}^6\text{He}, {}^5\text{He})d$ reaction in a CM angular range of 22° - 45° has been obtained from the energy spectrum of deuterons detected in coincidence with α particles.

Combined results of the three experimental runs are presented in Fig. 3a (elastic channel), Fig. 3b (${}^5\text{He} + d$ channel) and in Fig. 3c ($\alpha + t$ channel). Error bars include contributions from statistical errors and inaccuracy of efficiency simulations. The uncertainty of the absolute cross-section values is estimated to be within $\pm 20\%$ limit.

3. Analysis of the results

Apart from the present data, the angular distribution for the ${}^6\text{Li}(p, {}^3\text{He})\alpha$ reaction at 25 MeV proton beam ref. [11] are shown in Fig. 3c. These results were obtained at normal kinematics conditions. Under our convention, the CM scattering angle of inverse kinematics is defined as that of heavier reaction partner. This is, in fact, the recoiled particle angle that one obtains at normal kinematics, so the comparison the two angular distributions is straightforward. A simple inspection of data presented in Fig. 3c reveals significant differences between the two data sets. The two oscillations of the cross-section for the ${}^6\text{He}+p$ reaction are more pronounced, and their relative magnitudes are reversed in respect to the $p + {}^6\text{Li}$ data, though the average cross-sections values are close. On the ground of earlier studies of multi-nucleon transfer reactions, for example see [8,9,11] for ${}^6\text{Li} + p$, one should consider several direct mechanisms, which contribute in the reaction of ${}^6\text{He}+p \rightarrow \alpha + t$. Among one step processes the following mechanisms could be considered:

1. stripping of 2 neutrons from ${}^6\text{He}$ to p to form triton,
2. stripping of a 3-nucleon cluster as a triton, to form α particle,
3. knockout of α particle by proton,
4. knockout of triton by proton.

Among the two-step mechanisms the sequential stripping reaction of 2 neutron through the resonant $p_{3/2}$ and $p_{1/2}$ states of ${}^5\text{He}$ seems to be the most important. In a schematic view of direct reactions one could expect that processes 1 and 4 contribute to the cross-section at forward angles, whereas processes 2 and 3 are responsible for a rise of the cross-section at backward angles. Multi-step mechanisms, as well as various interference phenomena, could mostly contribute in the cross section at intermediate angles. It ought to be kept in mind, that in the finite range (FR) formalism with the proper core-core interaction included, the stripping and knockout processes are undistinguishable, thus processes (1) and (3) are united within one transfer reaction amplitude and similarly those (2) and (4). If one however assumes that the stripping processes are dominant in this energy region, then one could relate the cross section at forward angles to the α -2n clustering, whereas the reaction yield at backward angles could be associated with the $t+t$ clustering of ${}^6\text{He}$. In this naive picture the results shown in Fig. 3c suggest lower probability to find $t+t$ clusters in the ${}^6\text{He}$ nucleus than the ${}^3\text{He}+t$ clusters in the ${}^6\text{Li}$ nucleus. The shell model calculations predict just the opposite, see Table 1.

Table 1
Spectroscopic amplitudes (SA) for ${}^6\text{Li}$ and ${}^6\text{He}$ nuclei according to Ref. [6]

Nucleus	Configuration	State	SA
${}^6\text{Li}$	$\alpha + d$	$2S_1$	1.061
${}^6\text{He}$	$\alpha + 2n$	$2S_0$	1.0606
${}^6\text{Li}$	${}^3\text{He} + t$	$2S_{1/2}$	-0.9428
${}^6\text{He}$	$t + t$	$2S_{1/2}$	-1.333

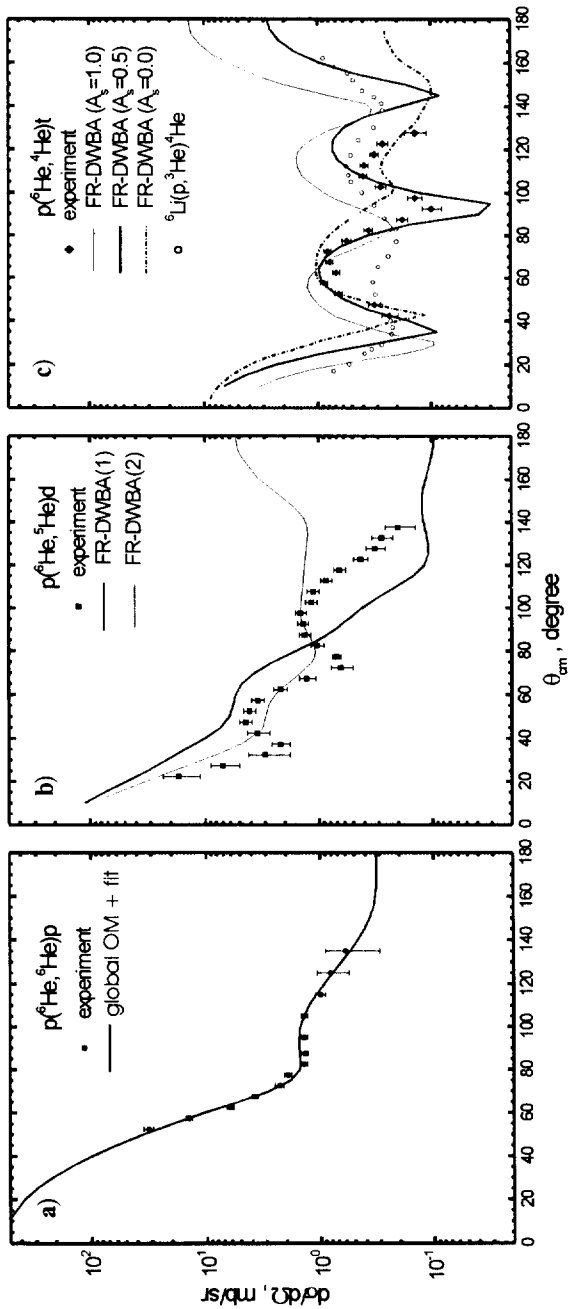


Fig. 3 Experimental data (symbols) and calculations (curves) of angular distributions: a) elastic scattering, b) $p(^6\text{He}, ^5\text{He})d$ reaction for two exit-channel OM potentials: extrapolated from Ref. [15]-thick solid line (1) and from Ref. [9]- thin solid line (2), c) $p(^6\text{He}, \alpha)t$ reaction for relative triton spectroscopic amplitude (A_s): neglected - dot-dashed line, full - thin solid line, full, reduced by a factor of 2 - thick solid line.

In order to discuss our results in a more quantitative way we performed a one-step DWBA analysis of ${}^6\text{He}$ data. The coupled channels (CC) code FRESKO [12] has been used in the first iteration which made it equivalent of multi-channel, finite range DWBA. Four processes were included in the calculation: elastic scattering, one-neutron transfer to the ${}^3\text{He}$ ground state and two-neutron and triton transfers, both leading to the $\alpha+t$ exit channel. In order to carry out the DWBA calculation the following ingredients are required for each transfer process.

1. Scattering wave functions for the entrance and exit channels. The wave functions were created by the use of appropriate optical model (OM) potentials.
2. Wave functions of the exchanged cluster-to-core relative motion for two bound states.
3. Interaction potential for the exchanged cluster.

In the simplified approach presented here the three-body internal wave functions relevant for the two-neutron transfer were substituted by two-body wave functions. These are ground-state wave functions produced in the usual way by the single-particle binding potentials. The interaction potential includes, as a main part, the binding potential completed by the potential of core-core interaction and OM potential of appropriate reaction channel.

It is well known that the transfer-reaction cross section calculated in DWBA strongly depends on OM parameters. For the program input we, to a large extent, endeavored to use parameters from literature. The OM parameters for the ${}^6\text{He}+p$ entrance channel were obtained by fitting our data of elastic scattering starting from the global nucleon – nucleus OM potential parameterized in Ref. [13].

The modified parameters are following: real part: $V=44.26$ (50.23), $R=1.95$ (2.064), $a=0.612$ (0.69), surface imaginary part: $W_s=3.98$ (9.335), $R=2.85$ (2.0), $a=0.772$ (0.69) (parameters from Ref. [13] are in parentheses). V , W_s , R , and a stand, respectively, for two depths [MeV], total radii [fm] and diffuseness parameters. The fit is shown in Fig 3a.

The formulae of Ref. [13] were exploited also to obtain the real proton-core interactions (i.e.: $p-t$, $p-{}^3\text{He}$) needed for the remnants of the interaction potentials in the (${}^6\text{He},t$) and (${}^6\text{He},{}^3\text{He}$) reactions, respectively. The potential proton-core i.e. $p-\alpha$ interaction, for need of (${}^6\text{He},\alpha$) transfer reaction calculation was taken from Satchler et al. [14]. The OM parameters for ${}^3\text{He} + d$ channel were taken either from the analysis of reactions induced by 14.1 MeV neutrons on ${}^6\text{Li}$ [9] or extrapolated from 4-parameter family of deuteron potentials proposed by Kull [15] in his study of the (p,d) reaction with light nuclei at $E_p=33.6$ MeV. The extrapolated values are $V=84.0$, W_s (surface)=44.0, $R=1.71$, $a=0.79$. Impact of each of these potentials is shown in Fig.3b. Some of the binding potentials generating the internal wave functions were borrowed from Ref. [8], the binding potential for the $\alpha+2n$ wave function was taken from Ref. [5]. For the $\alpha + t$ exit channel, as a preliminary, we repeated the procedure exposed in Ref. [5].

In a purely single cluster approach, $t + t$ configuration of ${}^6\text{He}$ is neglected here a priori, the di-neutron one step transfer was calculated with a FR DWBA code [18]. At this stage of the calculation the entrance channel OM potential was that for $p + {}^6\text{Li}$ at $E_p=25.9$ MeV (Table 2 in Ref. [16]) and the OM potential for $\alpha + t$ exit channel was that of $\alpha + {}^3\text{He}$ from Ref. [8]. The result of the calculation is shown in Fig. 3c as a dot-dashed line. It can be seen that the first oscillation of the angular distribution is reproduced.

At the next stage the triton transfer was included and the shell model spectroscopic amplitudes incorporated. From compilation [17] we took the OM parameter family with $V=173.0$, relevant of ${}^4\text{He}$ scattered on ${}^3\text{He}$ at $E_\alpha=42$ MeV, as the exit channel potential.

The calculated α -particle angular distribution of the $p({}^6\text{He},\alpha)t$ reaction was stable in respect to the choice of post or prior DWBA representation and appeared to be insensitive to small variations of the binding potential radius. The calculated cross section (thin solid line in Fig. 3c) follows the experimental points at scattering angles in forward hemisphere and overestimates those in the backward one. In order to diminish the discrepancy, the shell-model spectroscopic amplitude for the $t + t$ partition of ${}^6\text{He}$ presented in Table 1 was reduced by a factor of 2. Resulting calculated

cross section for the combination of two stripping processes, i.e. $2n$ and t transfers is shown in Fig. 3c as thick solid line.

Conclusions

For the first time the cross sections of elastic scattering and one- and two-neutron transfer reactions for the ${}^6\text{He} + p$ system were measured at 25 MeV/n collision energy in a wide angular range allowing a comparison with the analogous results for the ${}^6\text{Li} + p$ system [11]. An attempt was done to describe the new experimental results in the framework of a simplified version of finite range DWBA. The elastic scattering angular distribution was described by the fitting procedure starting from the global OM model. Two known OM potentials for the exit channel of $p({}^6\text{He}, {}^5\text{He})d$ reaction were used with a limited success, probably because they are appropriate to either higher or lower CM energy than in the present investigation. The $\alpha + t$ exit channel of the reaction studied is especially interesting since several mechanisms can contribute in its cross section. This reaction channel was treated as a sum of $2n$ - and t -transfer processes. Calculations incorporating shell model spectroscopic amplitudes for different ${}^6\text{He}$ partitions overestimate the cross section for this reaction in the region of large CM angles where the t -transfer process is supposed to play role. A better agreement with experimental data was obtained when the shell-model two-triton amplitude of ${}^6\text{He}$ was reduced by a factor of 2. This important conclusion should be still verified by a more sophisticated analysis involving also the treatment of the ${}^6\text{Li} + p$ data on equal footing. For that reason it is highly desirable to extend the experimental angular distribution to scattering angles smaller than 40° and/or to larger than 135° .

The work was carried out in the Flerov Laboratory of Nuclear Reactions of JINR. The partial support of this work by the Russian Basic Research Foundation (grant № 96-02-17382) is acknowledged. The authors are grateful to Drs. G. G. Gulbekian and B.N. Gikal for the valuable contribution to the production of a high quality, intense beam of ${}^{13}\text{C}$ ions. Fruitful discussions with Drs. J. Vaagen, Yu. M. Tchuvilski, N. Timofeyuk and N. Alamanos are very much appreciated.

References

1. I. Tanihata, J. Phys. G: Nucl. Part. Phys. 22 (1996) 157.
2. M.V. Zhukov et al., Phys. Rep. 231 (1993) 151.
3. M.J.G. Borge et al., Nucl. Phys. A560 (1993) 663.
4. D. Aleksandrov et al., Nucl. Phys. A633 (1998) 234.
5. G.M. Ter-Akopian et al., Phys. Lett. B426 (1998) 251.
6. O.F. Nemets et al., Appendix of "Nucleonic Associations in Atomic Nuclei and Nuclear Reactions of Multi-nucleon Transfer", Kiev 1988 (in Russian).
7. Yu.G. Mashkarov et al., Izv. RAN, Ser. Fiz. 59 (1995) 176 (in Russian).
8. M.F. Werby et al., Phys. Rev. C8 (1973) 106.
9. S.I. Higuchi et al., Nucl. Phys. A384 (1982) 51.
10. A. M. Rodin et al., Nucl. Inst. Meth. B126 (1997) 236.
11. K. Schenk et al., Phys. Lett. B52 (1974) 36.
12. I.J. Thompson, Computer Phys. Rep. 7 (1988) 167.
13. R.L. Varner et al., Phys. Rep. (1991) 57.
14. G.R. Satchler et al., Nucl. Phys. A112 (1968) 1.
15. L.A. Kull, Phys. Rev. 163 (1967) 1066.
16. K.H. Bray et al., Nucl. Phys. A189 (1972) 35.
17. C.M. Perey and F.G. Perey, At. Data Nucl. Data Tab. 17, No 1, (1976).
18. V. I. Zagrebaev, private communication.

Received by Publishing Department
on October 16, 1998.

**SUBJECT CATEGORIES
OF THE JINR PUBLICATIONS**

Index	Subject
1.	High energy experimental physics
2.	High energy theoretical physics
3.	Low energy experimental physics
4.	Low energy theoretical physics
5.	Mathematics
6.	Nuclear spectroscopy and radiochemistry
7.	Heavy ion physics
8.	Cryogenics
9.	Accelerators
10.	Automatization of data processing
11.	Computing mathematics and technique
12.	Chemistry
13.	Experimental techniques and methods
14.	Solid state physics. Liquids
15.	Experimental physics of nuclear reactions at low energies
16.	Health physics. Shieldings
17.	Theory of condensed matter
18.	Applied researches
19.	Biophysics

Вольски Р. и др.

E15-98-284

Исследование реакций передачи $1n$ и $2n$ в системе ${}^6\text{He} + p$ при энергии 25 МэВ/нуклон для пучка ${}^6\text{He}$

Измерены угловые распределения продуктов реакций передачи $1n$ и $2n$ в системе ${}^6\text{He} + p$ при энергии 25 МэВ/нуклон для пучка ${}^6\text{He}$. Экспериментальные данные проанализированы в рамках приближения искаженных волн. Полученные результаты свидетельствуют о более низкой величине двухтритонной спектроскопической амплитуды ядра ${}^6\text{He}$ в сравнении с результатами модели оболочек.

Работа выполнена в Лаборатории ядерных реакций им. Г.Н.Флерова ОИЯИ.

Сообщение Объединенного института ядерных исследований. Дубна, 1998

Wolski R. et al.

E15-98-284

Study of $1n$ and $2n$ Transfer Reactions in ${}^6\text{He} + p$ System at 25 MeV/n Energy of ${}^6\text{He}$ Beam

Angular distributions for $1n$ and $2n$ transfer reactions were measured in ${}^6\text{He} + p$ system at 25 MeV/n. Experimental data were analyzed in frame of DWBA. The results suggest lower two-triton spectroscopic amplitude for ${}^6\text{He}$ nucleus as compared to shell model calculation.

The investigation has been performed at the Flerov Laboratory of Nuclear Reactions, JINR.

Communication of the Joint Institute for Nuclear Research. Dubna, 1998

Макет Т.Е.Попеко

Подписано в печать 12.11.98
Формат 60 × 90/16. Офсетная печать. Уч.-изд. листов 1,04
Тираж 290. Заказ 51005. Цена 1 р. 25 к.

Издательский отдел Объединенного института ядерных исследований
Дубна Московской области